**EFFECT OF HEAT TREATMENT ON CORROSION RESISTANCE OF Al-Ni-Mn EUTECTIC ALLOY IN 3.5% NaCl SOLUTION**

**\* Yusuf KAYGISIZ** [ID]

*Aksaray University, Technical Vocational School of Sciences, Electricity and Energy Department, Aksaray, TÜRKİYE*
yusufkaygisiz@aksaray.edu.tr

*Highlights*

- The corrosion performance of the heat treated sample at 570°C is the highest.

- The matrix (M) phase is in equilibrium with the gray (G), White (W) and eutectic (E) phases.

- Open circuit potential of the samples that were heat treated at 570°C and 600°C and non-heat treated samples were found to be -685 mV, -693 mV and -761 mV, respectively.

- α-Al Matrix phase in the Al-Ni-Mn alloy is preferentially dissolved in the non-heat treated and heat treated samples.

**\*Corresponding Author:** Yusuf Kaygısız, yusufkaygisiz@aksaray.edu.tr

# EFFECT OF HEAT TREATMENT ON CORROSION RESISTANCE OF Al-Ni-Mn EUTECTIC ALLOY IN 3.5% NaCl SOLUTION

## *Yusuf KAYGISIZ [iD]

*Aksaray University, Technical Vocational School of Sciences, Electricity and Energy Department, Aksaray, TÜRKİYE*
yusufkaygisiz@aksaray.edu.tr

**ABSTRACT**: In this study, the effects of solution heat treatment (SHT) on how the Al-Ni-Mn eutectic alloy reacts to corrosion were looked into. The composition of the Al-Ni-Mn eutectic alloy was chosen as Al–5.3%Ni–1.3%Mn (wt). In solution heat treatment, firstly, the samples were kept at 570°C and 600°C for 2 hours and quenched with water at room temperature. Then, artificial aging was carried out by keeping 0-2-4 and 8 hours at 180°C. The corrosion behavior of the alloy was investigated by immersion tests in a 3.5% NaCl solution and electrochemical methods such as Tafel polarization curves and Electrochemical Impedance Spectroscopy (EIS). According to the immersion test results, the heat treatment applied at 600°C took the alloy to the more noble side and further increased its corrosion resistance. The $\alpha$-Al matrix phase in the Al-Ni-Mn alloy system preferentially dissolves in untreated and heat-treated samples, and SEM images reveal the presence of corrosion pits. The corrosion performance of the heat-treated sample at 570°C is the highest. Heat treatment reduced the corrosion current density, indicating a lower corrosion rate and higher corrosion resistance. Also, the open circuit potential of the Tafel polarization curves of heat-treated and unheat-treated samples at 570°C and 600°C was found to be -685 mV, -693 mV and -761 mV, respectively. Similarly, the corrosion resistance of heat-treated and untreated samples at 570°C and 600°C was found to be 58 kΩ, 433 kΩ and 408 kΩ, respectively.

*Keywords: Aluminium alloys, $Al_9(Mn,Ni)_2$ phase, Corrosion resistance, Heat treatment*

## 1. INTRODUCTION

Aluminum alloys have found use in many areas, from automotive to aircraft. The electrochemical properties and corrosion potential of aluminum alloys are as important as knowing and developing their mechanical properties. Similarly, the components of the alloy, the intermetallic phases occurring in the microstructure, and the sizes and distributions of these phases are as important as the potential difference of aluminum alloys with other metals, and these affect both the structure and morphology of the resulting corrosion [1]. The corrosion resistance of aluminum increases as the metal's purity increases. The use of 99.8% and 99.9% pure aluminum is generally limited to applications requiring very high corrosion resistance or ductility [1].

The microstructure of aluminum alloys varies depending on the composition, casting methods and processes, and applied heat treatment processes. In terms of corrosion properties, the grain structure in the microstructure, the presence of intermetallic phases, dispersides, and precipitates are the dominant features [1]–[7]. Al-Ni eutectic alloys exhibit excellent fluidity, excellent feedability, and low susceptibility to hot tearing [8]. However, it exhibits high mechanical properties at high temperatures thanks to its thermally stable $Al_3Ni$ intermetallic phase [9]–[11]. It is stated that in Al-Ni alloys, depending on sample processing and annealing conditions, the first phase to be formed will be $Al_3Ni$ [12]–[14], AlNi[15] or $Al_9Ni_2$[11], [14], [16]. Zuogui Zhang et al. [2], in their study on the corrosion behavior of Al-5.4%Ni (wt) alloy, it was stated that preferential corrosion pits were formed in the Al phase area and that the more homogeneous and thinner $Al/Al_3Ni$ structure played a vital role in improving the corrosion resistance of the alloy. Similarly, Wislei R. Osório et al. [17], in their study on the electrochemical corrosion behavior of Al-5%Ni(wt) alloy powders in 0.05 M NaCl solution, they stated that samples with a finer structure

**\*Corresponding Author:** Yusuf KAYGISIZ, yusufkaygisiz@aksaray.edu.tr

approached the positive side more and had higher corrosion resistance. In another study, Engelbert H. Padilla et al. [18], in their study on the corrosion behavior of NiAl and Ni₃Al intermetallic in acid rain, stated that both intermetallic phases have similar corrosion potential.

Although manganese has a low solubility in aluminum, it increases the corrosion resistance of the alloy and can reduce the possible harmful effects of ferrous intermetallic phases. Additions of up to 1% manganese provide good corrosion resistance as well as high formability in the structure [1], [19], [20]. Junwei Fu and Kai Cui [3] examined the effect of different amounts of Mn addition and heat treatment on the corrosion resistance of the Al-Cu-Mg alloy in 3.5% NaCl solution and stated that the Mn content increased the corrosion resistance of the alloy. They found the Ecorr and values to be -1.536 and -1.143 V for the additions of 0.6 Mn and 1.2 Mn, respectively.

Within the scope of this information, the aim of this study is to examine the corrosion behavior of the Al-Ni-Mn eutectic alloy formed using high purity Al, Ni and Mn elements in 3.5% NaCl solution and its changes according to heat treatment processes. The solution heat treatment process will be carried out in two stages at different temperatures of 570°C and 600°C. Electrochemical methods such as immersion tests and Tafel polarization curves and Electrochemical Impedance Spectroscopy will be used to determine the corrosion properties of the heat treatment process.

## 2. MATERIALS AND METHODS

### 2.1. Heat Treatment Process and Microstructure Observation

With the help of the phase diagram [21] of the Al-Ni-Mn alloy system, the composition of the eutectic point was determined as Al-5.3%Ni-1.3%Mn (wt). Mondolfo stated that according to this phase diagram, the eutectic reaction should be in the form: $L \rightarrow (Al) + Al_3Ni + Mn_3NiAl_{16}$ [22].

The schematic representation of the Solution heat treatment (SHT) process steps in this study is given in Figure 1. First, the formed samples were kept at temperatures below the eutectic temperature, at 570°C and 600°C for 2 hours, and quenched in water at room temperature. Then, artificial aging was carried out by keeping 0-2-4 and 8 hours at 180°C (Figure 1.).
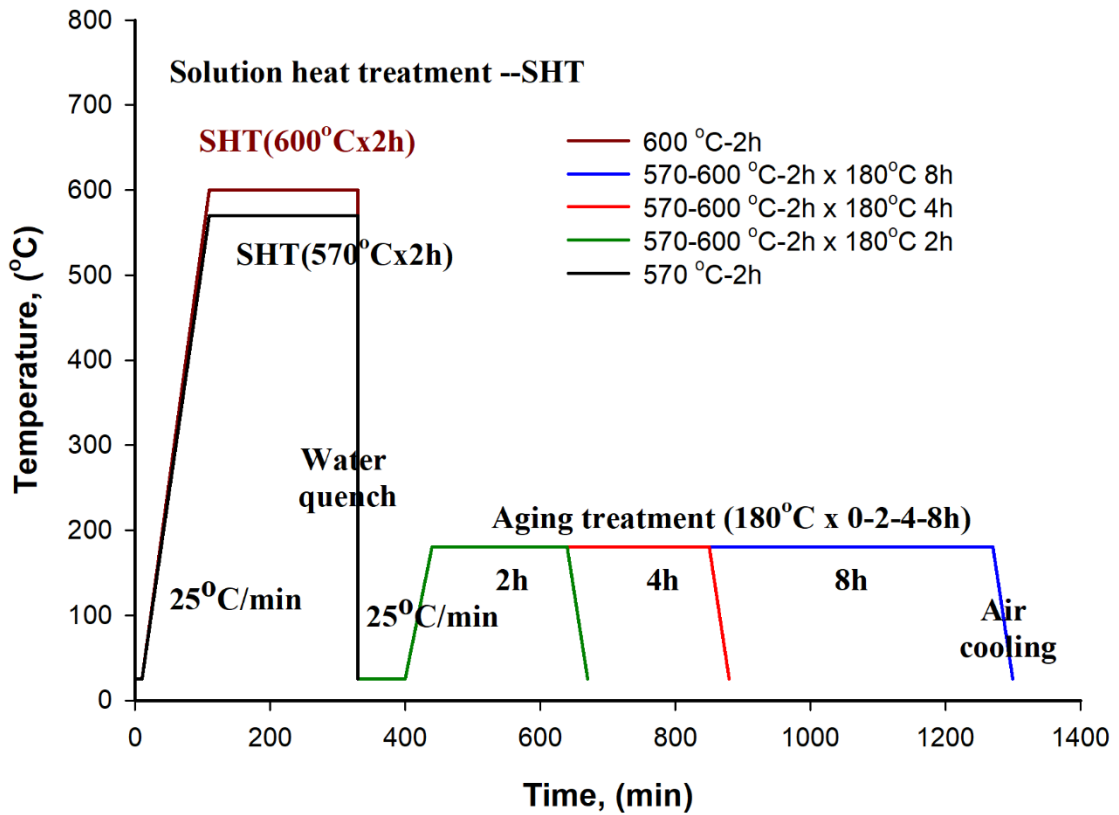
**Figure 1.** Schematic representation of solution heat treatment steps for Al-Ni-Mn alloy.

The typical SEM images of growth morphologies for eutectic Al-5.3wt%Ni-1.3wt.%Mn alloy are shown in Figure 2. As can be seen from Figure 2, the matrix (M) phase is in equilibrium with the gray (G), white (W) and eutectic (E) phases. According to the Energy dispersive spectroscopy (EDS) results given in Table 1, the $\alpha$-Al phase of the Matrix (M) phase, the gray phase's binary intermetallic $Al_9(Mn,Ni)_2$ phase and the white phase is $Al_3Ni$ intermetallic phase. Different from the phases indicated in the phase diagram [22], $Al_9(Mn,Ni)_2$ phase was observed. This metastable $Al_9Ni_2$ or $Al_9(Mn,Ni)_2$ phase was first described by Li and Kuo[23] in rapidly solidifying Al4Ni and Al6Ni alloys. Subsequently, precipitates were observed in the rapidly solidified Al-rich Al-Ni alloys[24], [25] and the annealed Al-rich Al/Ni alloys[26]. However, it should be noted that the $Al_9Ni_2$ phase does not occur in all Al-Ni alloys. We can say that the $Al_9Ni_2$ phase is the primary intermetallic phase at high solidification temperatures [27].
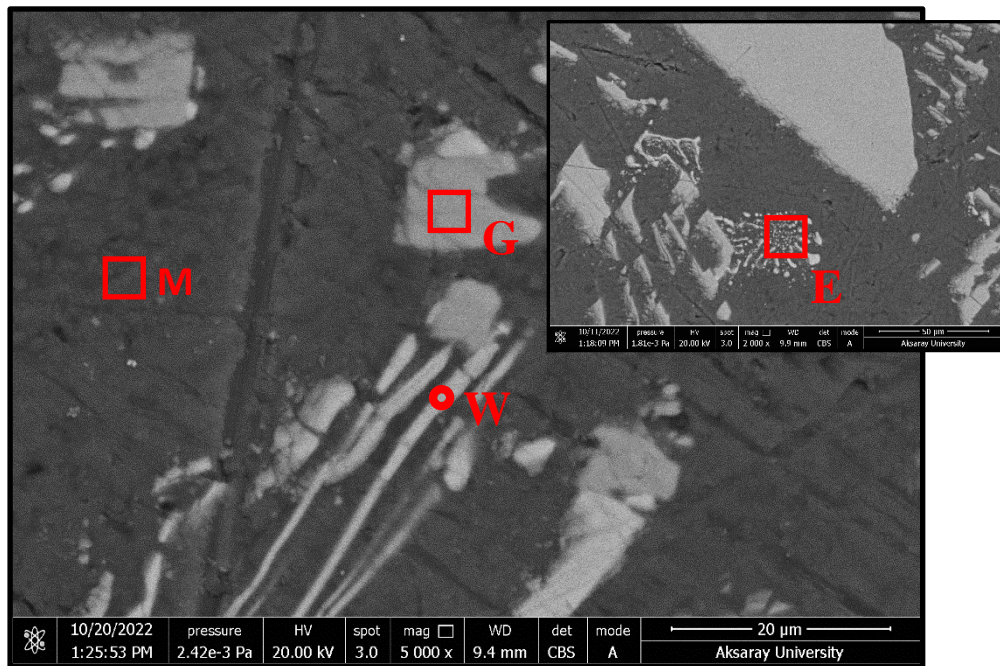
**Figure 2.** SEM image of longitudinal section of non-heat-treated Al-Ni-Mn alloy and, marked phase areas (M: Matrix phase, G: Gray phase, W: White phase, E: Eutectic area).

**Table 1.** EDS analysis results of the phases of Al-5.3Ni-1.3Mn (wt%) alloy before heat treatment.

| Process | Test area | Specific position | Al | | Ni | | Mn | |
|---|---|---|---|---|---|---|---|---|
| | | | wt. % | at.% | wt. % | at.% | wt. % | at.% |
| **Non-heat treated** | White | W | 61.48 | 77.63 | 37.87 | 21.97 | 0.65 | 0.40 |
| | Gray | G | 71.32 | 84.35 | 27.05 | 14.70 | 1.64 | 0.95 |
| | Matrix | M | 98.95 | 99.50 | 0.58 | 0.27 | 0.47 | 0.23 |
| | Eutectic | E | 88.50 | 94.36 | 11.15 | 5.46 | 0.35 | 0.18 |

### 2.2. Immersion Tests

Chlorides cause serious problems in metals or alloys due to their presence in many environments such as sea water and road salt, and in the chemical industry[28]. Therefore, in this study, mass loss measurements of Al-5.3%Ni-1.3%Mn (wt) alloy system prepared in eutectic composition were carried out in 3.5% NaCl solution at 25$^{\circ}$C' room temperature. Firstly, samples measuring 25 x 5 x 5 mm were cut, then they were mechanically polished using 360-600-1200-2000 and 4000 grit sandpaper and cleaned with deionized water. For mass loss measurement of heat treated and untreated alloy samples, they were kept in 3.5% NaCl solution at 25°C for 6-240 hours and the mass difference was measured with the help of precision balance. In order to remove the oxide layer and particle residues on the samples before weighing, they were kept in 10% silver nitrate ($AgNO_3$) prepared with distilled water for 30 seconds and then in 20% nitric acid ($HNO_3$) prepared with distilled water for 30 seconds.

The material removal rate or corrosion rate, which is an important corrosion parameter, can be expressed as the corrosion penetration rate (CPR) or the thickness loss of the material per unit time[29]. CPR can be formulated [29] as follows;

$$CPR = \frac{K.\Delta W}{\varphi.A.h} \tag{1}$$

where *ΔW* value is weight loss in mg, $\varphi$ is the density of the sample (calculated as $\varphi = 2.67\text{g/cm}^3$), *A* is the total surface area of the sample (cm²), *h* is the immersion time (hours). Since CPR is expressed in millimeters per year (mm/year), the *K* coefficient was taken as 87.6 [29].

## 2.3. Electrochemical Measurements

Corrosion measurements of Al-Ni Mn alloy were investigated using Tafel polarization curves and Nyquist diagrams obtained from Electrochemical Impedance Spectroscopy (EIS). Experimental studies were carried out using a conventional three-electrode cell in a 3.5% NaCl solution at room temperature. The Tafel polarization curves of the alloy samples were obtained at a scanning rate of 1mV/s (ν). Nyquist diagrams obtained by EIS method were measured in the range of 0.1 Hz to 100 kHz and at 10mV AC voltage amplitude.

## 3. RESULTS AND DISCUSSIONS

### 3.1. Effect of Heat Treatment on Corrosion Behaviors

### 3.1.1. Analysis of immersion test results

Mass loss measurements of heat-treated and non-heat-treated samples were performed by immersing them in 3.5% NaCl solution between 6 and 240 hours, and the graph showing the variation of corrosion rate/mass loss with immersion time is given in Figure 3. As can be seen from Figure 3, it can be said that for all samples, the corrosion progression rate progresses rapidly during the first 24 hours of immersion, while it progresses steadily (horizontal speed) in the subsequent processes. In other words, the corrosion kinetics (progression rate) in the first 24 hours decreased from 0.8520 to 0.2982, from 1.086 to 0.3054 and from 0.3208 to 0.1604 (mm/year) for the untreated samples and the samples heat treated at 570 and 600°C, respectively.
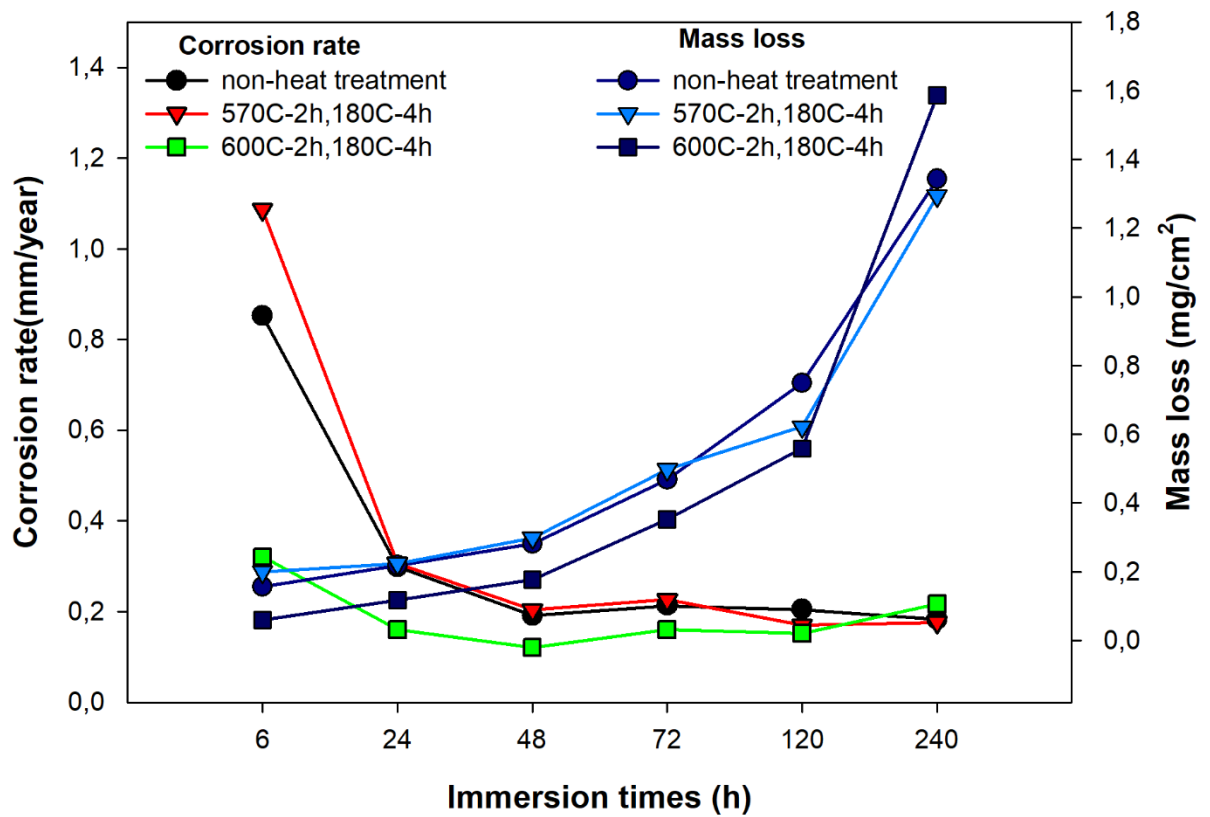
**Figure 3.** Immersion time& Corrosion rate and Mass loss curve for heat-treated and non-heat-treated Al-Ni-Mn alloy in 3.5% NaCl solution at 25ºC.

Again from Figure 3, it can be seen that the corrosion progression rate of the samples heat treated at 600ºC is lower than the corrosion progress rate of the samples that were non-heat treated and heat treated at 570ºC. Similarly, looking at the mass loss graph given in Figure 3, the mass loss increases exponentially with increasing immersion times for heat treated and non-heat treated samples. We can say that the heat treatment process applied at 600ºC takes the alloy to the more noble side and increases the corrosion resistance more.
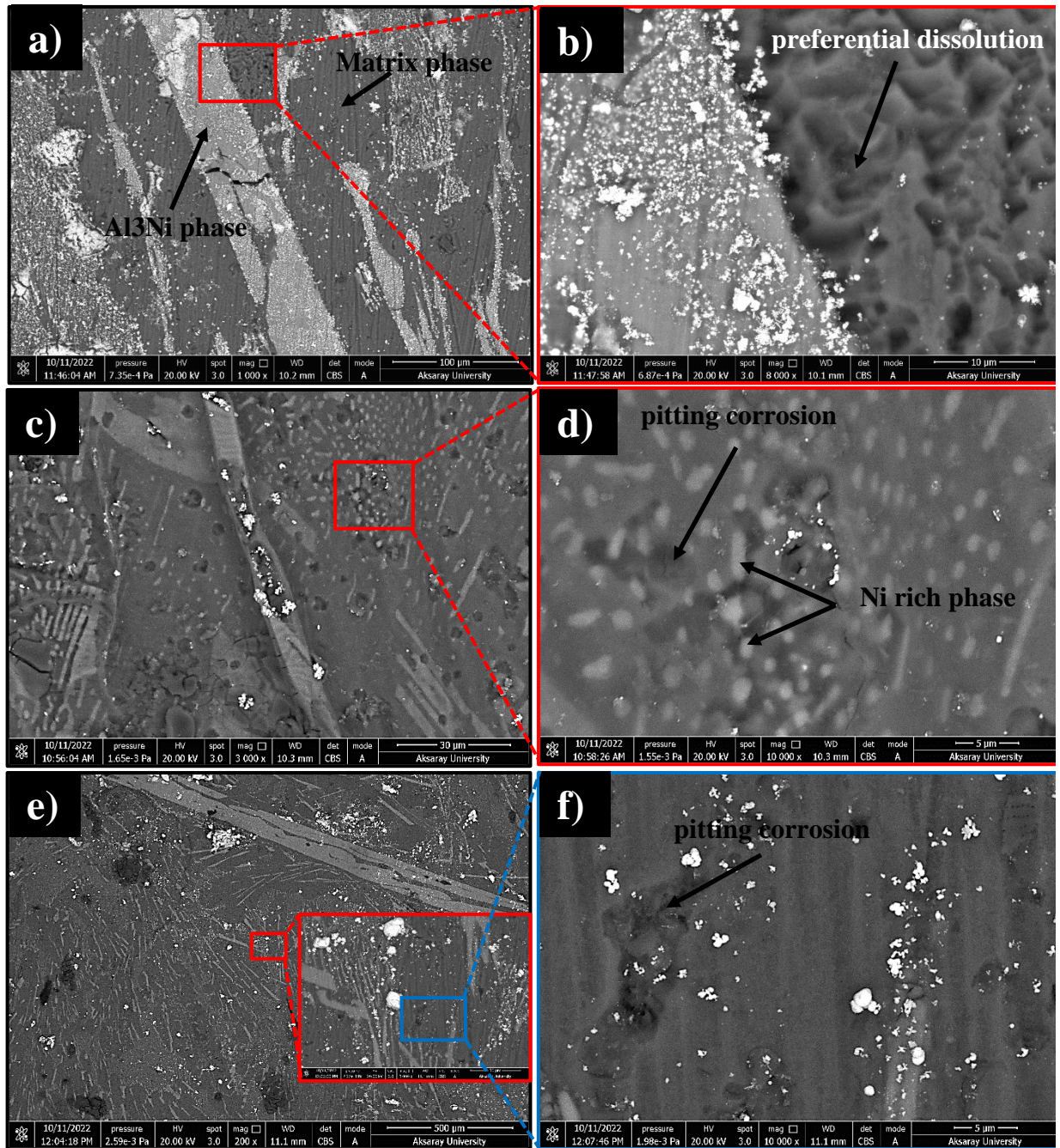
**Figure 4.** SEM images and corrosion types of samples immersed in 3.5% NaCI solution (a) not heat treated and immersed for 48 hours, (c) 2 hours at 570°C solution heat treated, then 4 hours at 180°C artificially aged and immerged for 48 hours, (e) 2 hours at 600°C solution heat treated, then 4 hours at 180°C artificially aged and immerged for 4 hours.

For determine the corrosion types after the immersion tests for corrosion progression rate/mass loss measurement, as shown in Figure 4, SEM images were taken from the heat treated and non-heat treated samples. As seen from the SEM images, the α-Al Matrix phase in the Al-Ni-Mn alloy system is preferentially dissolved in the non-heat treated and heat-treated samples. The SEM images given in Figure 4.d-f of the samples heat treated at 570°C and 600°C and immersed in NaCl solution for 48 hours reveal the presence of corrosion pits. It is worth noting that as can be seen from Figure 4.c-e, the heat treatment processes lead to a smaller Al matrix attack and corrosion pits.

Pitting corrosion [1], [30], [31] progression steps can be divided into several steps. In the 1st stage there are processes that lead to the breakdown of passivity. In stages 2 and 3, the early and late stages of pit growth and the final stage are repassivation. In stages 2 and 3, aluminum is oxidized to aluminum ions at the bottom of the pits. The reduction of water or hydrogen occurs in contact with the metal outside the pit. In both reduction reactions, the pH will increase outside the pit, giving an alkaline pH. The aluminum ions will create a film of aluminum chloride or aluminum oxychloride in the pit and stabilize it. After some time, aluminum chloride hydrolyzes to aluminum hydroxide. This causes the pH value to drop to a more acidic environment, which increases the corrosion rate in the furnace. Aluminum hydroxide precipitates at the edge of the pit and closes the opening, eventually inhibiting ion exchange and slowing down the corrosion process [28].
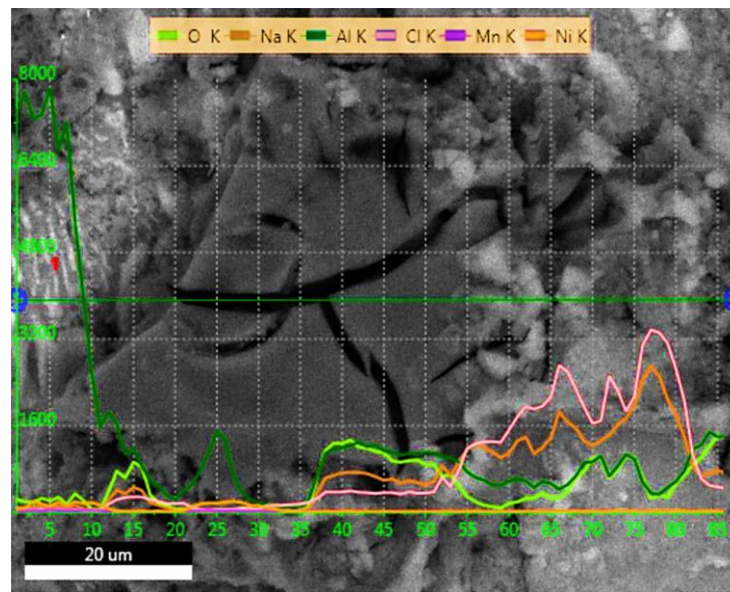


**Figure 5.** Line EDS image taken from the heat treated sample (solution heat treatment at 570°C for 2 hours, then artificial aging at 180°C for 4 hours) after immersion in 3.5% NaCl solution for 48 hours.

Line EDS and Mapping images taken from the sample (solution at 570°C for 2 hours, artificial aging at 180°C for 4 hours) immersed in 3.5% NaCl solution for 48 hours are shown in Figure 5 and Figure 6. These line EDS and mapping images also support preferential dissolution of the Al matrix phase. Shape. As can be clearly seen from the results of the line EDS given in Figure 5, an oxide layer has formed on the surface of the corrosion zone and CI- ions have accumulated around this oxide layer.
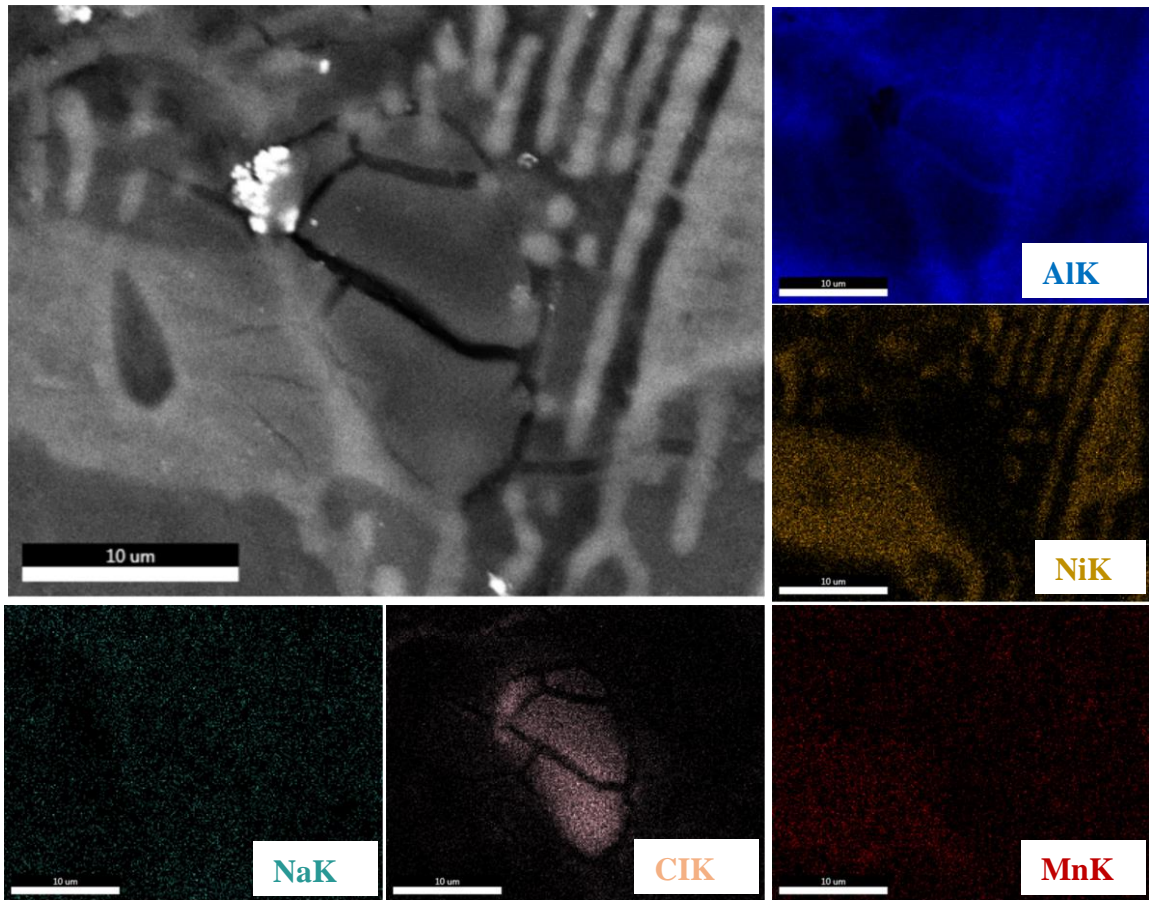
**Figure 6.** Mapping images of the heat treated sample (solution heat treatment at 570°C for 2 hours, then artificial aging at 180°C for 4 hours) immersed in 3.5% NaCl solution for 48 hours.

### 3.2. Analysis of electrochemical measurement results

Tafel polarization curves of heat treated and non-heat treated samples of Al-Ni-Mn eutectic alloy are given in Figure 7, and Nyquist diagrams obtained by Electrochemical Impedance Spectroscopy (EIS) method are given in Figure 8.

The corrosion characteristics of the alloys were determined by calculating the anodic and cathodic potentials in the Tafel area, together with their corresponding current densities. The corrosion current density ($i_{corr}$), which is directly related to the corrosion rate, was determined using the extrapolation of the cathodic and anodic Tafel lines to the corrosion potential ($E_{corr}$). The data shown in Figure 7 demonstrates that the non-heat-treated sample exhibits the greatest corrosion rate and a larger negative corrosion potential. Following the heat treatment conducted at temperatures of 570°C and 600°C, significant reductions in the corrosion rate were observed, accompanied by a change in the corrosion potential towards more positive values. The heat-treated sample exhibits the maximum corrosion performance when subjected to a temperature of 570°C. Furthermore, it can be seen that the application of heat treatment resulted in a decrease in the corrosion current density, so suggesting a reduction in the corrosion rate and an enhancement in the overall corrosion resistance.
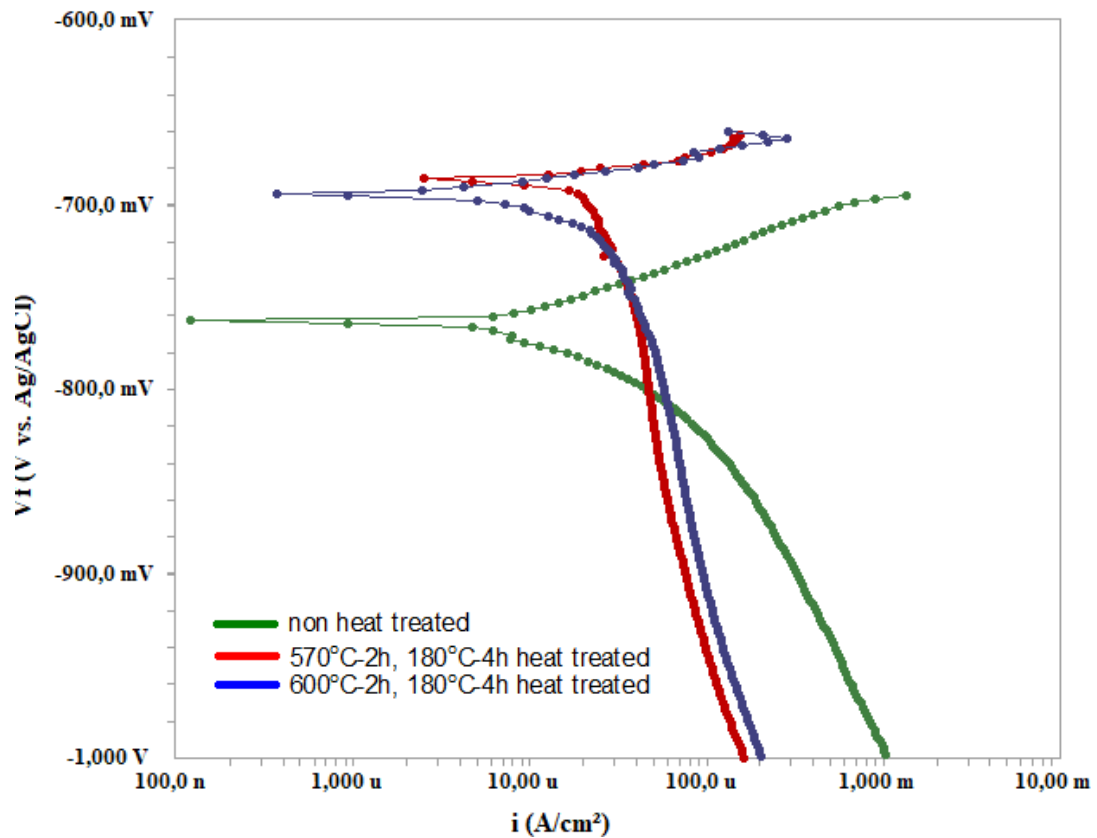
**Figure 7.** Current-Potential (Tafel polarization) curves recorded in 3.5% NaCl solution of Al-Ni-Mn eutectic alloys at a scanning rate of ʘ=1mV/s.

In addition, the open circuit potential of the Tafel polarization curves of the samples that were heat treated at 570ᵒC and 600ᵒC (2 hours in solution, then artificially aged at 180ᵒC for 4 hours) and non-heat treated samples were found to be -685 mV, -693 mV and -761 mV, respectively.

Nyquist diagrams obtained using EIS are given in Figure 8. The impedance data of the alloys were analyzed using Nyquist plots plotted against the imaginary part of the impedance ($-Z_{imag}$) versus the real part ($Z_{reel}$). Nyquist plots consist of a semicircle for all non-heat-treated and heat-treated samples. The magnitude of the semicircle represents the value of the charge transfer resistance ($R_{ct}$) [32], [33] existing between the electrode material and the corrosive ions present in the electrolyte. The broader semicircle denotes a favored corrosion tendency or increased impedance.
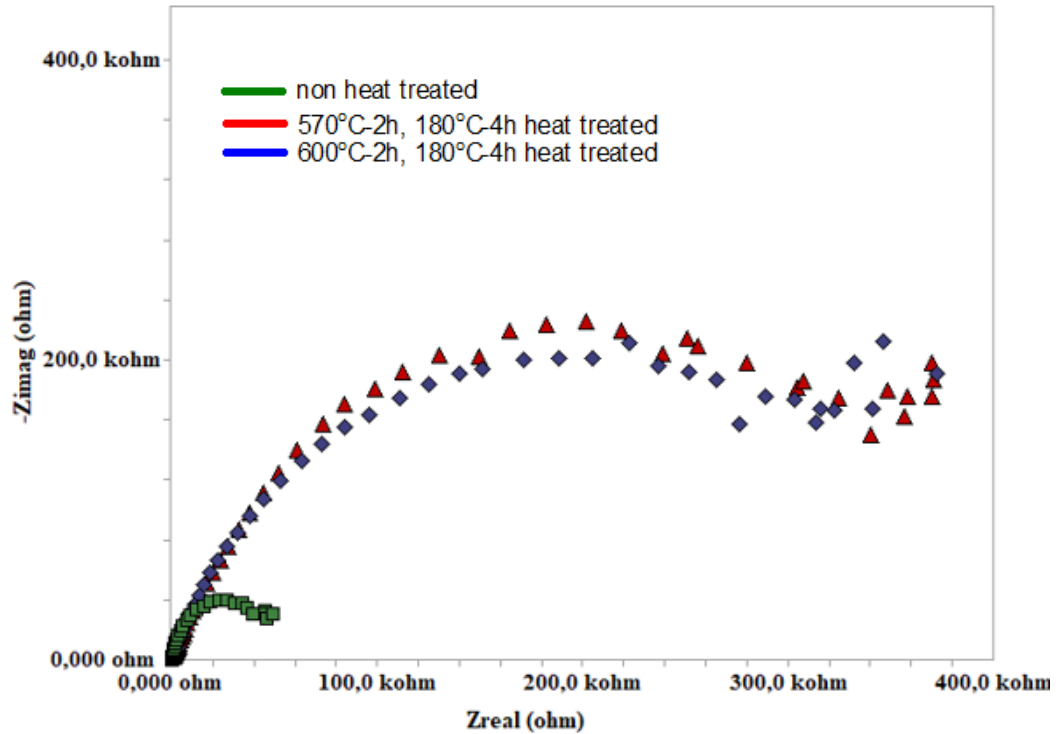
**Figure 8.** Nyquist plots obtained in 3.5% NaCl solution of Al-Ni-Mn eutectic alloy at -1.3V, frequency range: 0.1Hz-100kHz.

As can be seen from Figure 8, the non-heat treated sample has the lowest semicircular diameter (58k$\Omega$) compared to the heat treated samples. This result shows that a homogeneous structure is formed during the heat treatment process and this leads to a better corrosion resistance. With solution heat treatment at 570°C and 600°C, the corrosion resistance of Al-Ni-Mn alloy samples increased to 433 k$\Omega$ and 408 k$\Omega$, respectively. These results are consistent with those from the Tafel curves.

The findings derived from the implementation of Nyquist diagrams by the electrochemical impedance spectroscopy (EIS) technique and Tafel polarization curves have been consolidated and presented in Table 2. The findings demonstrate that heat treatment facilitated an increase in the corrosion potential, resulting in more positive values, and concurrently reduced the corrosion current density. As a result, the heat treatment process increased the corrosion resistance and decreased the corrosion rate.

**Table 2.** Corrosion potentials, corrosion current density and corrosion resistance of Al-Ni-Mn alloy

| Samples | Electrochemical measurement results | | |
|---|---|---|---|
| | $E_{corr}$/mV | $i_{corr}$/mA.cm$^{-2}$ | $R_{ct}$ /k $\Omega$ |
| Non-heat treated | -764 | $1.12 \times 10^{-1}$ | 58 |
| Heat treated (570°C)* | -682 | $1.63 \times 10^{-3}$ | 433 |
| Heat treated (600°C)** | -793 | $2.01 \times 10^{-3}$ | 408 |

$R_{ct}$: charge transfer resistance, *570°C-2h-180°C-4h, **600°C-2h-180°C-4h

The immersion test results and electrochemical measurement results performed to determine the corrosion behavior of Al-Ni-Mn eutectic alloy were compared with the experimental results of similar studies in the literature [2], [3], [36]–[38], [6], [17]–[20], [28], [34], [35]. Zuogui Zhang et al.[2], in their study investigating the corrosion behavior of Al-5.4%Ni (wt) alloy produced by equal channel angular pressing (ECAP), they stated that preferential corrosion pits were formed in the Al phase area. It has also been stated that the more homogeneous and thinner Al/Al₃Ni structure plays a vital role in improving the

corrosion resistance of the Al-5.4% Ni (wt.) alloy. Wislei R. Osório et al. [17], in their study investigating the electrochemical corrosion behavior of Al-5%Ni(wt) alloy powders in 0.05 M NaCl solution, they stated that samples with finer microstructure approached the positive side more and had higher corrosion resistance. In the same study, the open circuit potentials of Tafel polarization curves were found to be -647 mV and -729 mV. These results are in full agreement with the open circuit potentials (685 mV, -693 mV and -761 mV) found in our study. Engelbert H. Padilla et al.[18], in their study investigating the corrosion behavior of NiAl and $Ni_3Al$ intermetallics in acid rain, stated that both intermetallic phases have similar corrosion potential. They found the $E_{corr}$ and $I_{corr}$ values for $Ni_3Al$ intermetallic to be -339.21 mV/SCE and $0.54 \times 10^{-3}$ mA/cm$^2$, respectively. These values are approximately half of the $E_{corr}$ and $I_{corr}$ values given in Table 2, which we found in our study for samples heat treated at 570$^o$C and 600$^o$C. This may be due to the difference in the immersed solution. Junwei Fu and Kai Cui[3], examined the effects of different amounts of Mn addition and heat treatment on the corrosion resistance in 3.5% NaCl solution on the Al-Cu-Mg alloy. In their study, they found that the addition of Mn to the Al-Cu-Mg alloy had a significant effect on the electrochemical corrosion parameters. The addition of Mn increased the corrosion resistance of the alloy. For the additions of 0.6 Mn and 1.2 Mn, they found the $E_{corr}$ and values to be -1.536 V and -1.143 V, respectively. Similarly, they measured $I_{corr}$ values as $3.388 \times 10^{-4}$ A/cm$^2$ and $7.197 \times 10^{-6}$ A/cm$^2$ for 0.6 Mn and 1.2 Mn additions, respectively. They reported that they observed that corrosion resistance increased with the heat treatment process in the precipitation hardening heat treatment, in parallel with the results obtained in our study. In another study, Donghui Zhang and Dejun Kong[38], in their study investigating the effect of Al-Ni coating on S355 steel in 3.5% NaCl solution on corrosion resistance, stated that increasing the Ni ratio in Al increases the corrosion resistance of the alloy. In the amorphous Al-Ni coating with a 4:1 mass ratio of Al and Ni, the $E_{corr}$ and $I_{corr}$ values were found to be -0.727 V and 0.0028 A/m$^2$, respectively. This value is in full agreement with the experimental results obtained in our study for the sample heat treated at 600 $^o$C

## 4. CONCLUSIONS

The typical SEM images of growth morphologies for eutectic Al-5.3wt%Ni-1.3wt.%Mn alloy are shown in Figure 2. As can be seen from Figure 2, the matrix (M) phase is in equilibrium with the gray (G), white (W) and eutectic (E) phases. According to the Energy dispersive spectroscopy (EDS) results given in Table 1, the α-Al phase of the Matrix (M) phase, the gray phase's binary intermetallic $Al_9(Mn,Ni)_2$ phase and the white phase is $Al_3Ni$ intermetallic phase. Different from the phases indicated in the phase diagram [22], $Al_9(Mn,Ni)_2$ phase was observed. Despite these observed phases, the $Mn_3NiAl_{16}$ (Q) phase, which is one of the phases in the reaction expected in the eutectic composition, was not found in the SEM and EDS images. It is thought that the $Mn_3NiAl_{16}$ (Q) phase, which Mondolfo's claims to be in the eutectic reaction, is due to the solidification rate not allowing this phase to form.

According to the SEM images taken from the samples after the immersion tests in 3.5% NaCl solution, it is clearly seen that the α-Al Matrix phase in the Al-Ni-Mn alloy system is preferentially dissolved in the non-heat treated and heat treated samples.

In the immersion test results, it is seen that the corrosion progression rate of the samples heat treated at 600$^o$C is lower than the corrosion progress rate of the samples that were not heat treated and heat treated at 570$^o$C. In contrast, for heat-treated and non-heat-treated samples, the mass loss increases exponentially with increasing immersion times.

The Tafel curves reveal that the non-heat-treated sample exhibits the greatest corrosion rate and has greater negative corrosion potential. Following the application of heat treatment at temperatures of 570°C and 600°C, a significant reduction in the corrosion rate was seen, accompanied with a change in the corrosion potential towards more positive values. The open circuit potential of the Tafel polarization curves of the samples that were heat treated at 570$^o$C and 600$^o$C (2 hours in solution, then artificially aged at 180$^o$C for 4 hours) and non-heat treated samples were found to be -685 mV, -693 mV and -761 mV, respectively.

Nyquist diagrams drawn by Electrochemical Impedance Spectroscopy and Tafel curves were observed to be consistent. The non-heat treated sample has the lowest semicircular diameter (58kΩ) compared to the heat treated samples. The obtained outcome demonstrates the formation of a homogenous structure by the heat treatment procedure, resulting in increased corrosion resistance. The corrosion resistance of the samples was enhanced to 433 kΩ and 408 kΩ, respectively, after heat treatment at temperatures of 570ºC and 600ºC.

According to the findings obtained from Nyquist diagrams and Tafel polarization curves and summarized in Table 2, it shows that heat treatment increases the corrosion potential and reaches more positive values. The heat treatment process also reduced the corrosion current density. As a result, the heat treatment process increased corrosion resistance and reduced the corrosion rate.

### Declaration of Competing Interest

The authors declare that they have no known competing financial interests or personal relationships that could have appeared to influence the work reported in this paper.

### Funding / Acknowledgements

### REFERENCES

[1]     G. M. Scamans, N. Birbilis, and R. G. Buchheit, "Corrosion of aluminum and its alloys," in *Corrosion of Aluminum and its Alloys*, 2010, pp. 1974–2010.

[2]     Z. Zhang, E. Akiyama, Y. Watanabe, Y. Katada, and K. Tsuzaki, "Effect of $\alpha$-Al/Al3Ni microstructure on the corrosion behaviour of Al-5.4 wt% Ni alloy fabricated by equal-channel angular pressing," *Corros. Sci.*, vol. 49, no. 7, pp. 2962–2972, 2007.

[3]     J. Fu and K. Cui, "Effect of Mn content on the microstructure and corrosion resistance of Al-Cu-Mg-Mn alloys," *J. Alloys Compd.*, vol. 896, p. 162903, 2022.

[4]     M. C. Reboul, T. J. Warner, H. Mayet, and B. Baroux, "A ten-step mechanism for the pitting corrosion of aluminium," *Mater. Sci. Forum*, vol. 217–222, no. PART 3, pp. 1553–1558, 1996.

[5]     R. G. Buchheit, "A Compilation of Corrosion Potentials Reported for Intermetallic Phases in Aluminum Alloys," *J. Electrochem. Soc.*, vol. 142, no. 11, pp. 3994–3996, 1995.

[6]     Yusuf Kaygısız and Didem Balun Kayan, "Effect of Heat Treatment on the Mechanical Properties and Corrosion Behaviour of Al–Si–Mg Alloy Systems," *Phys. Met. Metallogr.*, vol. 123, no. 14, pp. 1499–1508, 2022.

[7]     Ş. Candan, S. Çim, S. Emir, and E. Candan, "AZ91 Mg Alaşımlarında Korozyon Davranışı-Fe Tolerans Sınırı Arasındaki İlişkinin Araştırılması," *Konya J. Eng. Sci.*, vol. 7, no. 3, pp. 654–662, 2019.

[8]     N. A. Belov, A. N. Alabin, and D. G. Eskin, "Improving the properties of cold-rolled Al-6%Ni sheets by alloying and heat treatment," *Scr. Mater.*, vol. 50, no. 1, pp. 89–94, 2004.

[9]     C. Suwanpreecha, P. Pandee, U. Patakham, and C. Limmaneevichitr, "New generation of eutectic Al-Ni casting alloys for elevated temperature services," *Mater. Sci. Eng. A*, vol. 709, no. September 2017, pp. 46–54, 2018.

[10]    J. T. Kim, S. H. Hong, J. M. Park, J. Eckert, and K. B. Kim, "Microstructure and mechanical properties of hierarchical multi-phase composites based on Al-Ni-type intermetallic compounds in the Al-Ni-Cu-Si alloy system," *J. Alloys Compd.*, vol. 749, pp. 205–210, 2018.

[11]    F. Yousefi, R. Taghiabadi, and S. Baghshahi, "Effect of Partial Substitution of Mn for Ni on Mechanical Properties of Friction Stir Processed Hypoeutectic Al-Ni Alloys," *Metall. Mater. Trans. B Process Metall. Mater. Process. Sci.*, vol. 49, no. 6, pp. 3007–3018, 2018.

[12]    E. Ma, M. A. Nicolet, and M. Nathan, "NiAl3 formation in Al/Ni thin-film bilayers with and

without contamination," *J. Appl. Phys.*, vol. 65, no. 7, pp. 2703–2710, 1989.

[13]  E. Ma, C. V. Thompson, and L. A. Clevenger, "Nucleation and growth during reactions in multilayer Al/Ni films: The early stage of Al3Ni formation," *J. Appl. Phys.*, vol. 69, no. 4, pp. 2211–2218, 1991.

[14]  A. S. Edelstein, R. K. Everett, G. R. Richardson, S. B. Qadri, J. C. Foley, and J. H. Perepezko, "Reaction kinetics and biasing in Al/Ni multilayers," *Mater. Sci. Eng. A*, vol. 195, no. C, pp. 13–19, 1995.

[15]  R. B. and K. B. C. Mıchaelsen, S. Wohlert, "The Early Stages of Solid-State Reactions In Ti/Al Multilayer Films," *Eff. Partial Substit. Mn Ni Mech. Prop. Frict. Stir Process. Hypoeutectic Al-Ni Alloy.*, vol. 398, pp. 245–250, 1996.

[16]  M. H. Da Silva Bassani, J. H. Perepezko, A. S. Edelstein, and R. K. Everett, "Initial phase evolution during interdiffusion reactions," *Scr. Mater.*, vol. 37, no. 2, pp. 227–232, 1997.

[17]  W. R. Osório, J. E. Spinelli, C. R. M. Afonso, L. C. Peixoto, and A. Garcia, "Electrochemical corrosion behavior of gas atomized Al-Ni alloy powders," *Electrochim. Acta*, vol. 69, pp. 371–378, 2012.

[18]  E. H. Padilla, A. M. Flores, C. A. Ramírez, I. A. López, and L. B. Gómez, "Electrochemical corrosion characterization of nickel aluminides in acid rain," *Rev. Mater.*, vol. 23, no. 2, 2018.

[19]  C. Cao, D. Chen, J. Ren, J. Shen, L. Meng, and J. Liu, "Improved strength and enhanced pitting corrosion resistance of Al-Mn alloy with Zr addition," *Mater. Lett.*, vol. 255, p. 126535, 2019.

[20]  H. Mraied, W. Cai, and A. A. Sagüés, "Corrosion resistance of Al and Al–Mn thin films," *Thin Solid Films*, vol. 615, pp. 391–401, 2016.

[21]  V. S. Zolotorevsky, N. A. Belov, and M. V. Glozoff, *Plating Aluminium Alloys.* Amsterdam: Elsevier Ltd., 2007.

[22]  Mondolfo L F., *Aluminum Alloys-Structure and Properties*. 1976.

[23]  X. Z. Lit and K. H. Kuo, "Decagonal quasicrystals with different periodicities along the tenfold axis in rapidly solidified al-ni alloys," *Philos. Mag. Lett.*, vol. 58, no. 3, pp. 167–171, 1988.

[24]  J. F. Nie and B. C. Muddle, "Microstructure in rapidly solidified Al-Ti-Ni alloys," *Mater. Sci. Eng. A*, vol. 215, no. 1–2, pp. 92–103, 1996.

[25]  C. Pohla and P. L. Ryder, "Crystalline and quasicrystalline phases in rapidly solidified Al-Ni alloys," *Acta Mater.*, vol. 45, no. 5, pp. 2155–2166, 1997.

[26]  A. Yamamoto and H. Tsubakino, "Al9Ni2 precipitates formed in an Al-Ni dilute alloy," *Scr. Mater.*, vol. 37, no. 11, pp. 1721–1725, 1997.

[27]  M. A. Martínez-Villalobos *et al.*, "Microstructural evolution of rapid solidified Al-Ni alloys," *J. Mex. Chem. Soc.*, vol. 60, no. 2, pp. 67–72, 2016.

[28]  J. Tao, "'Surface composition and corrosion behavior of an Al-Cu alloy,'" Docteur De L'université Pierre Et Marie Curie, 2016.

[29]  J. A. D. G. R. Wıllıam D. Callıster, *Materials Science and Engineering an Introduction*, 9th ed. Wiley, 2013.

[30]  T. Suter and R. C. Alkire, "Microelectrochemical Studies of Pit Initiation at Single Inclusions in Al 2024-T3," *J. Electrochem. Soc.*, vol. 148, no. 1, p. B36, 2001.

[31]  R. L. Cervantes, L. E. Murr, and R. M. Arrowood, "Copper nucleation and growth during the corrosion of aluminum alloy 2524 in sodium chloride solutions," *J. Mater. Sci.*, vol. 36, no. 17, pp. 4079–4088, 2001.

[32]  D. Balun Kayan, D. Koçak, and M. İlhan, "Electrocatalytic hydrogen production on GCE/RGO/Au hybrid electrode," *Int. J. Hydrogen Energy*, vol. 43, no. 23, pp. 10562–10568, 2018.

[33]  D. B. Kayan, M. İlhan, and D. Koçak, "Chitosan-based hybrid nanocomposite on aluminium for hydrogen production from water," *Ionics (Kiel).*, vol. 24, no. 2, pp. 563–569, 2018.

[34]  Y. Yang *et al.*, "Improved corrosion behavior of ultrafine-grained eutectic Al-12Si alloy produced by selective laser melting," *Mater. Des.*, vol. 146, pp. 239–248, 2018.

[35]  D. S. Carvalho, C. J. B. Joia, and O. R. Mattos, "Corrosion rate of iron and iron-chromium alloys in CO2 medium," *Corros. Sci.*, vol. 47, no. 12, pp. 2974–2986, 2005.

[36]  M. jia Li *et al.*, "Improved intergranular corrosion resistance of Al-Mg-Mn alloys with Sc and Zr additions," *Micron*, vol. 154, no. December 2021, p. 103202, 2022.

[37]  M. Mirzaee-Moghadam *et al.*, "Dry sliding wear characteristics, corrosion behavior, and hot deformation properties of eutectic Al–Si piston alloy containing Ni-rich intermetallic compounds," *Mater. Chem. Phys.*, vol. 279, no. January, p. 125758, 2022.

[38]  D. Zhang and D. Kong, "Microstructures and immersion corrosion behavior of laser thermal sprayed amorphous Al-Ni coatings in 3.5 % NaCl solution," *J. Alloys Compd.*, vol. 735, pp. 1–12, 2018.